Available online at www.sciencedirect.com

ScienceDirect

www.elsevier.com/locate/brainres

Brain Research

Research Report

Targeting alpha-synuclein with a microRNA-embedded silencing vector in the rat substantia nigra: Positive and negative effects

*Christina E. Khodr, Amanda Becerra, Ye Han, Martha C. Bohn**

Department of Pediatrics, Neurobiology Program, Ann and Robert H. Lurie Children's Hospital of Chicago Research Center, Feinberg School of Medicine, Northwestern University, 225 E. Chicago Ave., Box 209, Chicago, IL 60611, United States

ARTICLE INFO

Article history:
Accepted 10 January 2014
Available online 21 January 2014

Keywords:
Neurodegeneration
RNAi
Substantia nigra
Gene therapy
Tyrosine hydroxylase

ABSTRACT

Background: Alpha-synuclein (SNCA) downregulation shows therapeutic potential for synucleinopathies, including Parkinson's disease (PD). Previously we showed that human (h)SNCA gene silencing using a short hairpin (sh)RNA in rat substantia nigra (SN) protects against a hSNCA-induced forelimb deficit, but not dopamine (DA) neuron loss. Furthermore, the shRNA increases cell death *in vitro*, but the same target sequence embedded in a microRNA30 transcript (mir30-hSNCA) does not. *Objective*: Examine hSNCA gene silencing using mir30-hSNCA *in vivo*. *Methods*: Rats were stereotaxically injected into one SN with adeno-associated virus serotype 2/8 (AAV)-hSNCA, AAV-hSNCA plus AAV-mir30-SNCA or AAV-hSNCA plus a control non-silencing mir30-embedded siRNA and DA neuron markers and associated behavior were examined. *Results*: AAV2/8-mediated SN hSNCA expression induces a forelimb deficit and tyrosine hydroxylase-immunoreactive (TH-IR) neuron loss. hSNCA gene silencing using mir30-hSNCA protects against this forelimb deficit at 2 m and ameliorates TH-IR neuron loss. Striatal (ST) TH-IR fiber density and DA markers, assessed by western blot, are unaffected by AAV-hSNCA alone. Co-expression of either silencing vector reduces ST TH-IR fibers, panTH in SN and Ser40 phosphorylated TH in SN and ST, but does not affect vesicular monoamine transporter-2. However, hSNCA gene silencing promotes partial TH-IR fiber recovery by 2 m. Co-expression of either silencing vector also induces SN inflammation, although some recovery was observed by 2 m in hSNCA-silenced SN. *Conclusion*: hSNCA gene silencing with AAV-mir30-hSNCA has positive effects on forelimb behavior and SN DA neurons, which are compromised by inflammation and reduced TH expression, suggesting that AAV2/8-mir30-hSNCA-mediated gene silencing, although promising *in vitro*, is not a candidate for therapeutic translation for PD.

**Corresponding author*. Fax: +1 773 755 6344.
E-mail addresses: m-bohn@northwestern.edu, b-corstange@northwestern.edu (M.C. Bohn).

0006-8993
http://dx.doi.org/10.1016/j.brainres.2014.01.010

1. Introduction

Aberrant expression of alpha-synuclein (SNCA) occurs in a number of diseases termed synucleinopathies, including Parkinson's disease (PD), multiple system atrophy and dementia with Lewy bodies (Marti et al., 2003). In familial forms of PD, SNCA is directly associated with disease pathogenesis due to three missense mutations in the SNCA gene or multiplication of the gene (Lee and Trojanowski, 2006). SNCA is further implicated in the pathogenesis of sporadic PD because it is a major protein component of intra-cytoplasmic inclusions termed Lewy bodies, a diagnostic hallmark of PD (Spillantini et al., 1997). These findings suggest that therapeutically targeting aberrant SNCA expression may ameliorate disease pathogenesis in both sporadic and familial PD.

Many SNCA-based experimental models of PD have been created in an effort to better understand the role of SNCA in disease pathogenesis. Transgenic mouse models of PD in which SNCA is expressed under the control of various promoters allowing expression in a ubiquitous or cell-specific manner have been created. These mice vary in that some do not display symptoms and others display varying degrees of motor behavioral deficits and/or dopamine (DA) neuron degeneration in the substantia nigra (SN), which also is a hallmark of PD pathogenesis (Chesselet, 2008). Rat models of PD in which human (h) SNCA is experimentally expressed in the SN using viral vectors also have been created. In these rats, loss of DA neurons occurs over a short time frame offering advantages for therapeutic studies (Kirik et al., 2002, 2003; Lo Bianco et al., 2002). A rat model of PD in which hSNCA is delivered to the rat SN using an adeno-associated viral vector (AAV), similar to the one originally characterized by Kirik's group (Kirik et al., 2002), was used in the current study.

RNA interference (RNAi) is an evolutionarily conserved process of gene regulation involving double-stranded RNA mediated degradation or translational inhibition of homologous mRNAs (Fire et al., 1998; Scherr and Eder, 2007). This RNAi process can be utilized as a therapeutic approach to reduce expression of genes associated with disease. Several different approaches have been taken to reduce aberrant SNCA expression in rodent models of PD, including use of ribozymes (Hayashita-Kinoh et al., 2006), intracellularly-expressed single chain antibodies (Yuan and Sierks, 2009), small inhibitory RNAs (Lewis et al., 2008; McCormack et al., 2010), short hairpin (sh) RNAs (Sapru et al., 2006), microRNAs (mir) (Han et al., 2011) and most recently, mirtrons (Sibley et al., 2012) that target SNCA. In the current study, a mir-embedded siRNA was used to reduce aberrant expression of hSNCA in a rat model of PD.

We previously observed that expression of an shRNA specific for hSNCA protects against a forelimb motor deficit induced by ectopic expression of hSNCA in rat SN. However, an accompanying loss of DA neurons in the SN was also observed (Khodr et al., 2011). Toxicity due to expression of an shRNA has been observed in other studies in various cell types, including neurons (Boudreau et al., 2008, 2009; Castanotto et al., 2007; Grimm et al., 2006; McBride et al., 2008; Yi et al., 2005). *In vitro*, this hSNCA-specific shRNA also reduces survival of DA PC12 cells. However, toxicity of this shRNA in PC12 cells is eliminated by embedding the silencing sequence in a mir30 transcript (Han et al., 2011). This finding is in line with the findings of McBride et al. who showed safer silencing when an initially toxic shRNA sequence is embedded in a mir30 backbone (McBride et al., 2008). To further develop our SNCA gene silencing approach for PD, here we report *in vivo* results testing the less toxic mir30-embedded hSNCA-specific silencing vector (mir30-SNCA) in rat SN.

2. Results

2.1. Optimizing AAV-hSNCA to AAV-mir30-SNCA ratio

An initial dose study was performed to determine the optimal ratio of AAV2/8-hSNCA to AAV2/8-mir30-SNCA, to verify expression of hSNCA in the rat SN and identify a dose of AAV2/8-hSNCA that reproduces the deficit in ipsilateral forelimb use previously reported for AAV2/2-hSNCA (Khodr et al., 2011). Three AAV-hSNCA doses and six AAV-mir30-SNCA vector doses were injected unilaterally into the SN together or separately (Table S1), and the rats were assessed for levels of hSNCA expression, TH-immunoreactive (IR) cell counts at one level of SN and forelimb paw use at 1 month.

After injection of AAV-hSNCA, a dose dependent level of expression of hSNCA-IR was observed in soma and fibers in ipsilateral SN and ventral tegmental area (VTA) and in fibers in ipsilateral striatum (ST) (Fig. 1a). A dose dependent significant loss of TH-IR neurons in these rats was also observed (Table S1). Reduced contralateral forelimb use was observed at the lowest dose (0.6×10^{10} vg) of AAV-hSNCA (Fig. 1b).

When different ratios of mir30-SNCA were examined, hSNCA-IR was found to be reduced in rats that received the lowest dose of mir30-SNCA (1:3 ratio), although hSNCA expression was still detectable in cell bodies in the SN and in fibers in both SN and ST. At the highest dose of mir30-SNCA (1:55 ratio), hSNCA-IR was not detected in ST and only rare hSNCA-IR cells or fibers were detected in the SN, although a diffuse background of hSNCA-IR was observed in the SN (Fig. 1a). A statistically significant protection from the AAV-hSNCA-induced deficit in contralateral forelimb use was observed at a hSNCA to mir30-SNCA ratio of 1:55, but not at a ratio of 1:29 or 1:3 in this pilot study with $n=3$ (contra: $F_{5,12}=3.8$, $p=0.0275$; ipsi: $F_{5,12}=6.2$, $p=0.0046$; Fig. 1b). However, no significant differences in numbers of TH-IR neurons between control and injected SN at any ratio of AAV-hSNCA to AAV-mir30-SNCA were found (Table S1). Because TH neuron counts do not differ between injected and control SN at any ratio of hSNCA to mir30-SNCA (Table S1), the optimal ratio was determined by the efficiency of hSNCA-IR silencing and the protection against the deficit in forelimb motor behavior, which differs among hSNCA to mir30-SNCA ratios. Based on the results of this pilot study, the subsequent efficacy experiments were carried out using the 1:55 hSNCA to mir30-SNCA ratio.

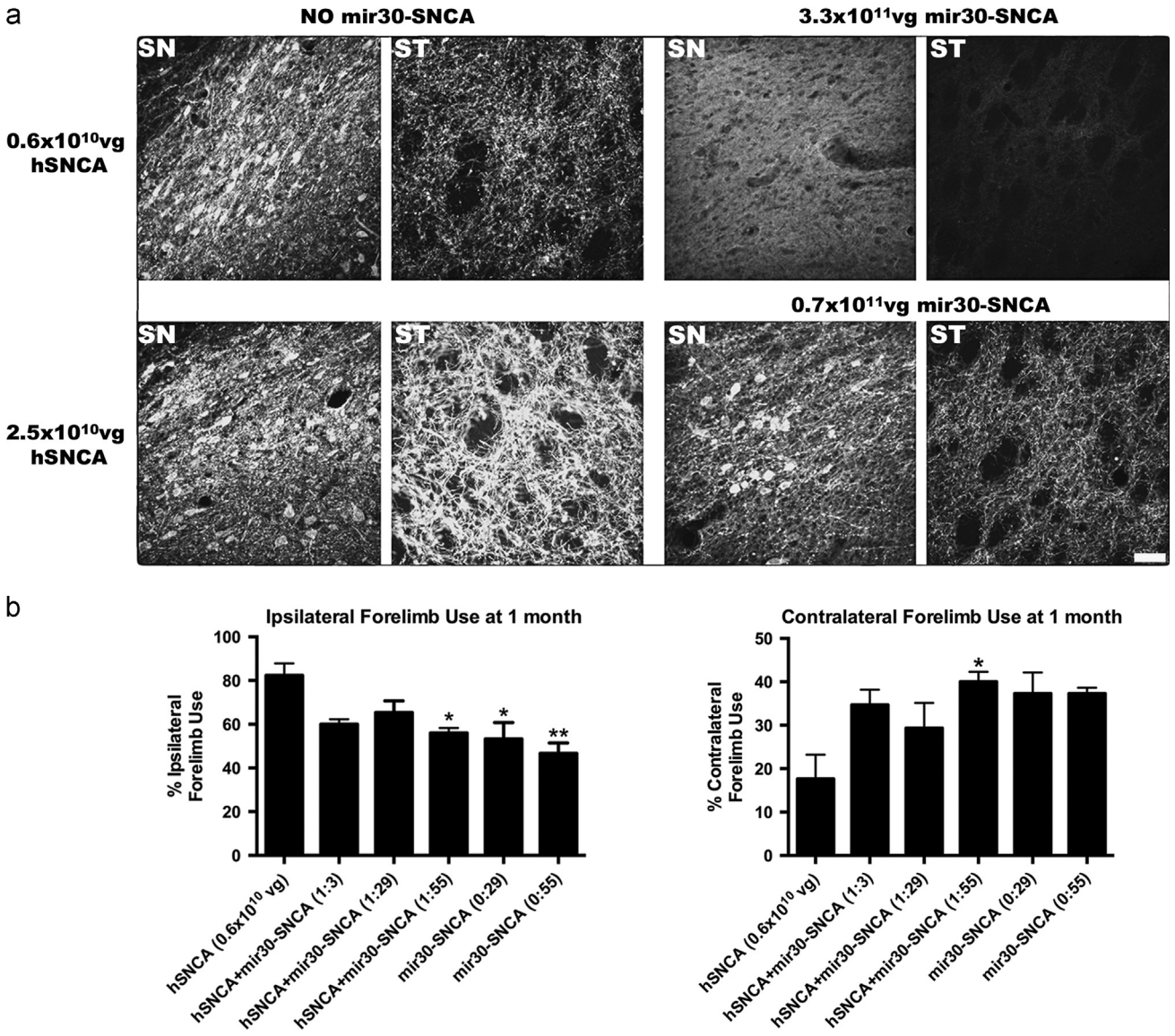

Fig. 1 – Efficiency of hSNCA gene silencing at different doses of AAV2/8-hSNCA and AAV2/8-mir30-hSNCA. Different doses of AAV2/8-hSNCA and ratios of AAV2/8-hSNCA to AAV2/8-mir30-hSNCA were injected into SN of rats to determine optimal doses and ratios to use for efficacy experiments. All doses and ratios tested are shown in Table S1. (a) Representative images showing expression of hSNCA at 1 month are shown for both the SN and ST of rats that were injected with the low dose (0.6×10^{10} vg, upper panel) or high dose (2.5×10^{10} vg, lower panel) of AAV8-hSNCA alone (left panels) or with AAV2/8-mir30-hSNCA (right panels) at a ratio of 1:3 (lower panels) or 1:55 (upper panels). At the 1:3 ratio, hSNCA expression in both neurons and fibers in SN and in fibers in ST is visibly reduced compared to the respective hSNCA alone group, but is still apparent. At the 1:55 ratio, hSNCA expression is barely detectable in either SN or ST. Images were taken at the same settings. Size bar: 50μm. Additional images that include hSNCA-IR for the 1:29 ratio of AAV8-hSNCA to AAV8-mir30-hSNCA are shown in Fig. S1. (b) Forelimb preference was tested using the cylinder test at 1 month after injection. Ipsilateral and contralateral forelimb use are shown from rats injected with the low dose of AAV2/8-hSNCA alone or with three different doses of silencing vector with (a ratio of 1:3, 1:29 or 1:55) or without AAV2/8-hSNCA (a ratio of 0:29 or 0:55). The number of times each paw was used on the first 25 rearings was counted and is expressed as a percentage of total paw use (mean ± SEM). Statistical differences compared to rats injected with hSNCA alone are as follows: $^{*}p \leq 0.05$; $^{**}p \leq 0.01$. hSNCA gene silencing significantly ameliorates the forelimb deficit observed in hSNCA-treated rats at the 1:55 hSNCA to silencing vector ratio. The 1:55 hSNCA to silencing vector ratio was chosen for the efficacy studies because hSNCA-IR is severely reduced and forelimb behavior is significantly ameliorated.

2.2. *hSNCA gene silencing in SN and ST*

To confirm that rats in each treatment group were transduced with the vectors to the same extent, DNA levels of hSNCA and turbo GFP (representing either mir30-SNCA or a control, non-silencing, silencing vector containing a scrambled target sequence (NS)) were determined by quantitative real time QPCR at 10d (Fig. S2a and b) and 2 months (Fig. 2a) survival in the

ventral midbrain. All groups received similar levels of hSNCA vector DNA (Fig. S2b and Fig. 2a). Groups injected with AAV-hSNCA and AAV-mir30-SNCA, or AAV-hSNCA and AAV-NS, received similar levels of silencing vector DNA, as measured by turbo GFP (Fig. S2a). hSNCA DNA also was detected in the ST of rats that received AAV-hSNCA alone, but not in ST from other treatment groups (Fig. S3).

hSNCA expression levels were examined at the mRNA level in the ventral midbrain and ST at 10d (Fig. S2c) and 2 months (Fig. 2b and c) using qRT-PCR to confirm hSNCA expression and silencing. hSNCA mRNA levels are significantly reduced in rats injected with AAV-hSNCA and AAV-mir30-SNCA compared to rats injected with AAV-hSNCA alone at both the level of the ventral midbrain ($p \leq 0.05$; $F_{5,24}=20.77$, $p<0.0001$; Fig. 2b) and the ST ($p \leq 0.001$; $F_{5,24}=285.5$, $p<0.0001$; Fig. 2c). hSNCA mRNA levels also are reduced in ST injected with AAV-hSNCA and AAV-mir30-SNCA compared to those injected with AAV-hSNCA and AAV-NS ($p \leq 0.001$, $F_{5,24}=285.5$, $p<0.0001$; Fig. 2c). However, hSNCA RNA levels in ventral midbrain injected with AAV-hSNCA and AAV-mir30-SNCA do not differ from those in ventral midbrain injected with AAV-hSNCA and AAV-NS. These data suggest that hSNCA mRNA and vector DNA, in the case of injection of AAV-hSNCA alone, are transported to the ST.

2.3. *hSNCA gene silencing protects against a hSNCA-induced deficit in forelimb motor behavior*

To examine effects of hSNCA expression and silencing in the SN on motor behavior, forelimb behavior was examined using the cylinder test 1 and 2 months after unilateral SN injection of AAV-hSNCA, AAV-hSNCA and AAV-mir30-SNCA or AAV-hSNCA and AAV-NS (Fig. 3). As expected, a preference for ipsilateral forelimb use and a deficit in contralateral forelimb use was observed in rats expressing hSNCA (i.e., rats injected with AAV-hSNCA alone or AAV-hSNCA and AAV-NS) at both 1 month (hSNCA: $p \leq 0.01$, ipsi-77.9±4.2%, contra-21.1±3.9%, $n=16$; hSNCA and NS: $p \leq 0.01$, ipsi-69.3±3.1%, contra-26.4±2.0%, $n=15$; $F_{4,132}=11.78$, $p<0.0001$) and 2 months (hSNCA: $p \leq 0.05$, ipsi-77.5±6.2%, contra-22.5±6.2%, $n=11$; hSNCA and NS: $p \leq 0.05$, ipsi-80.0±3.1%, contra-18.8±3.3%, $n=10$; $F_{4,87}=18.69$, $p<0.0001$) after injection. hSNCA gene silencing with mir30-SNCA results in protection against the hSNCA-induced deficit in forelimb use by 2 months after injection, when ipsilateral and contralateral forelimb use does not statistically differ (ipsi-51.1±2.1%, contra-45.3±1.1%, $n=11$), although a preference ($p \leq 0.05$) for ipsilateral forelimb use (57.3±3.1%,$n=16$) and a deficit in contralateral forelimb use (37.3±2.8%) was observed at 1 month in rats where hSNCA was silenced with mir30-SNCA. The 2-way ANOVA showed no significant effect of time or interaction of time and treatment.

2.4. *Effect of hSNCA gene silencing on TH-IR neuron numbers*

SN brain sections from rats injected with AAV-hSNCA, AAV-hSNCA and AAV-mir30-SNCA or AAV-hSNCA and AAV-NS at 1 and 2 months survivals were stained for TH-IR. Qualitatively, SNs injected with AAV-hSNCA and AAV-NS have the most evident reduction in TH-IR, where TH-IR neurons were observed in smaller, narrower bands, at both survivals (Fig. S4a and Fig. 4a), compared with the other treatments. TH-IR neurons throughout the entire SN were counted using unbiased stereology at both 1 and 2 months (Fig. S4b and Fig. 4b). At 1 month, TH-IR neurons are reduced in hSNCA-expressing SN, (hSNCA: 8521±538, $p \leq 0.01$, $n=5$, and hSNCA and NS: 7557±642, $p \leq 0.001$, $n=5$) compared to the respective control SN (hSNCA: 12,116±290, $n=5$, and hSNCA+NS: 12,415 ±377, $n=5$), but are not significantly different in SN where hSNCA is silenced using mir30-SNCA (10,118±1290, $n=5$) compared to control SN (12,679±251, $n=5$; $F_{5,24}=10.72$, $p<0.0001$), suggesting protection of DA neurons by silencing of hSNCA. However, TH-IR cell counts are not statistically

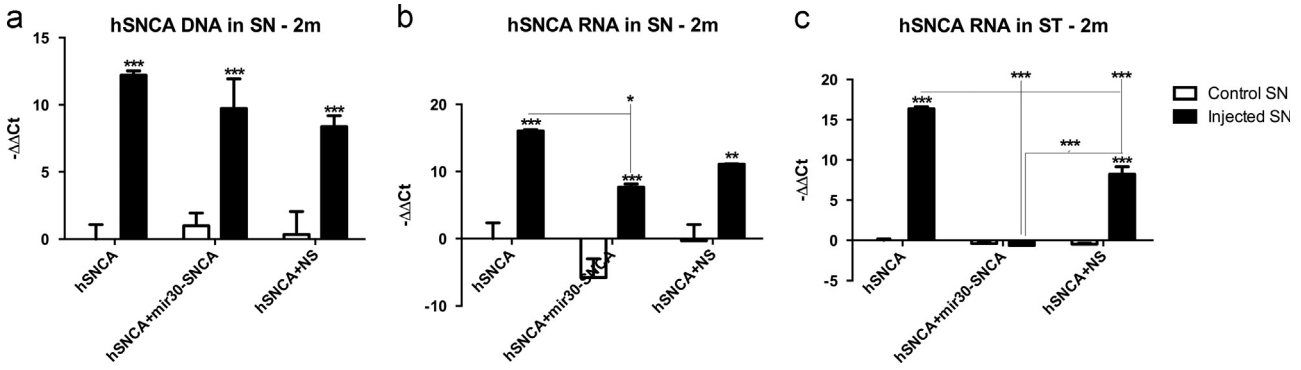

Fig. 2 – hSNCA gene silencing in the ventral midbrain and ST. hSNCA expression at the DNA and RNA levels was determined in rats unilaterally injected with AAV2/8-hSNCA or AAV2/8-hSNCA with either the AAV2/8-mir30-SNCA silencing vector or a non-silencing control vector (NS). Non-injected (control SN) and vector injected ventral midbrain and corresponding STs were dissected from rats and processed for qPCR and/or qRT-PCR. (a) hSNCA DNA in ventral midbrain, (b) hSNCA mRNA in ventral midbrain and, and (c) hSNCA mRNA in the ST. DNA and mRNA levels relative to β-actin mRNA are shown (mean±SEM). Asterisks represent statistical differences between control and injected SN unless otherwise noted (*$p \leq 0.05$; **$p \leq 0.01$; ***$p \leq 0.001$). Note that hSNCA mRNA levels are significantly reduced in both ventral midbrain and ST in rats injected with the specific mir30-hSNCA silencing vector. In contrast, the levels of hSNCA vector DNA remain high in injected midbrain of all treatment groups and neither the hSNCA-specific nor the NS silencing vectors significantly affect these levels.

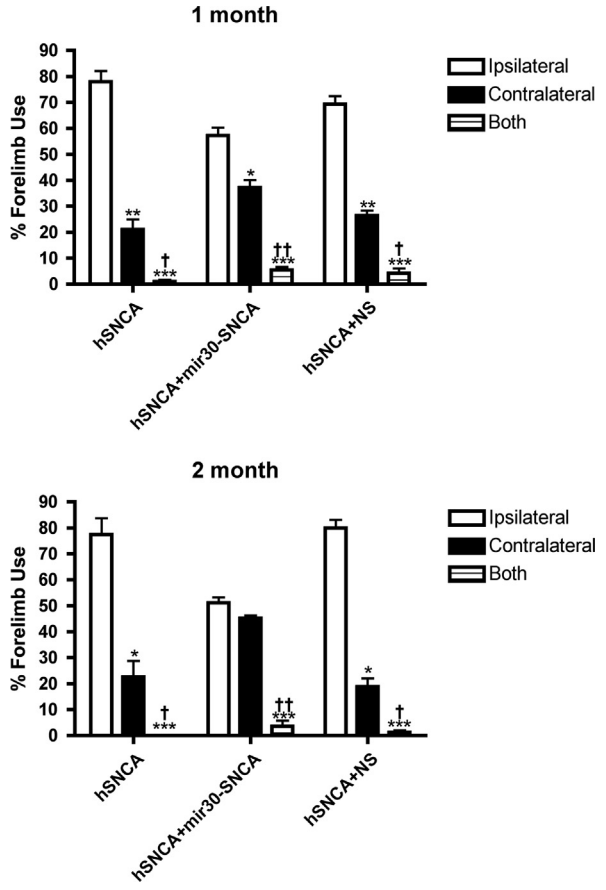

Fig. 3 – hSNCA gene silencing protects against a hSNCA-induced deficit in forelimb motor behavior. Rats were injected with AAV8-hSNCA alone or AAV8-hSNCA plus either AAV8-mir30-hSNCA or a non-silencing control vector (NS) into one SN. Forelimb preference was tested using the cylinder test at both 1 and 2 months after injection. The number of times each paw was used on the first 25 rearings was counted and is expressed as a percentage of total paw use (mean ± SEM). Statistical differences are shown for each treatment group as follows: differences compared to ipsilateral forelimb use ($^{*}p \leq 0.05$; $^{**}p \leq 0.01$; $^{***}p \leq 0.001$), and differences compared to contralateral forelimb use ($^{\dagger}p \leq 0.05$; $^{\dagger\dagger}p \leq 0.01$). At 1 month, all treatment groups show a preference for contralateral paw use apparently due to expression of hSNCA in the SN, although this deficit is less significant in the hSNCA silenced group. However, by 2 months, rats in which hSNCA is silenced recover and show no preference in paw use.

different in injected SNs of all treatment groups. At 2 months, TH-IR neuron numbers also are reduced ($p \leq 0.001$) in hSNCA-expressing SN (i.e. hSNCA: 8518 ± 586, $n=6$, and hSNCA and NS: 6466 ± 264, $n=5$) compared to respective control SN (hSNCA: 12,145 ± 204, $n=6$, and hSNCA and NS: 12,254 ± 262, $n=5$). SNCA gene silencing ameliorates this deficit in TH-IR neurons because rats where hSNCA was silenced with mir30-SNCA have a less severe reduction ($p \leq 0.05$) in the number of TH-IR neurons in the injected SN (10,355 ± 732, $n=6$) compared to the respective control SN (12,633 ± 213), and this reduction is not significant in comparison to the control SNs from the hSNCA-expressing groups. Injection of AAV-hSNCA and AAV-NS exacerbates the deficit in TH-IR neurons in that SNs injected with AAV-hSNCA and AAV-NS have reduced TH-IR neurons compared to SNs injected with AAV-hSNCA and AAV-mir30-SNCA, as well as those injected with AAV-hSNCA alone ($p \leq 0.05$ compared to hSNCA, $p \leq 0.001$ compared to hSNCA and mir30-SNCA; $F_{5,28}=28.90$, $p<0.0001$). Note that although significant differences were observed between treated SNs at 2 months, and not at 1 month, the pattern and magnitude of effects at 1 and 2 months are very similar and do not differ significantly between time points, which was verified by a lack of significant effect of time or interaction of time and treatment by 2-way ANOVA.

2.5. *Expression of either mir30-SNCA or NS silencing vector results in loss of total TH expression, without loss of VMAT2 in ventral midbrain*

To further examine effects of hSNCA expression and silencing on DA neurons in the SN, the ventral midbrain was dissected from rats injected with AAV-hSNCA, or AAV-hSNCA and either AAV-mir30-SNCA or AAV-NS silencing vector and endogenous rat DA phenotypic markers were examined at the mRNA and protein levels (Fig. 5). TH mRNA levels (Fig. 5a) are reduced in ventral midbrain injected with either AAV-mir30-SNCA or AAV-NS silencing vector compared to AAV-hSNCA-injected or control ventral midbrain, and this reduction is greatest in ventral midbrain injected with AAV-hSNCA and AAV-NS, which have reduced TH mRNA levels compared to all control ventral midbrains ($F_{5,24}=15.66$, $p<0.0001$). Protein levels follow this same trend in that ventral midbrain injected with either AAV-mir30-SNCA or AAV-NS silencing vector exhibit reduced TH protein using a pan TH antibody ($F_{5,24}=6.148$, $p=0.0008$; Fig. 5c), as well as Ser40 phosphorylated (P-Ser40) TH antibody (Fig. 5d), an activated form of TH, compared to AAV-hSNCA-injected and control ventral midbrain. However, control ventral midbrains from rats that received either silencing vector also show reduced P-Ser40 TH protein expression ($F_{5,24}=8.421$, $p=0.0007$). Interestingly, protein levels of vesicular monoamine transporter 2 (VMAT2, Fig. 5e) are not significantly affected by treatment, suggesting that expression of TH is selectively affected by silencing vector in DA neurons.

2.6. *Expression of either mir30-SNCA or NS silencing vector results in an initial loss of TH-IR fibers in the ST, which partially recovers after 2 months of hSNCA gene silencing*

ST brain sections from rats injected with AAV-hSNCA, AAV-hSNCA and AAV-mir30-SNCA or AAV-hSNCA and AAV-NS at 1 and 2 months survivals were stained for TH-IR. Qualitatively, ST co-injected with AAV-hSNCA and either AAV-mir30-SNCA or AAV-NS silencing vector have the most evident reductions in TH-IR at 1 month (Fig. 6a). By 2 months, TH-IR in ST injected with AAV-hSNCA and AAV-mir30-hSNCA exhibits recovery compared to the 1 month time point (Fig. 6b). The density of TH-IR fibers at the level of the anterior commissure was measured using NIH Image J at both 1 and 2 months (Fig. 6c and d). TH-IR fiber density measurements are not significantly affected by hSNCA

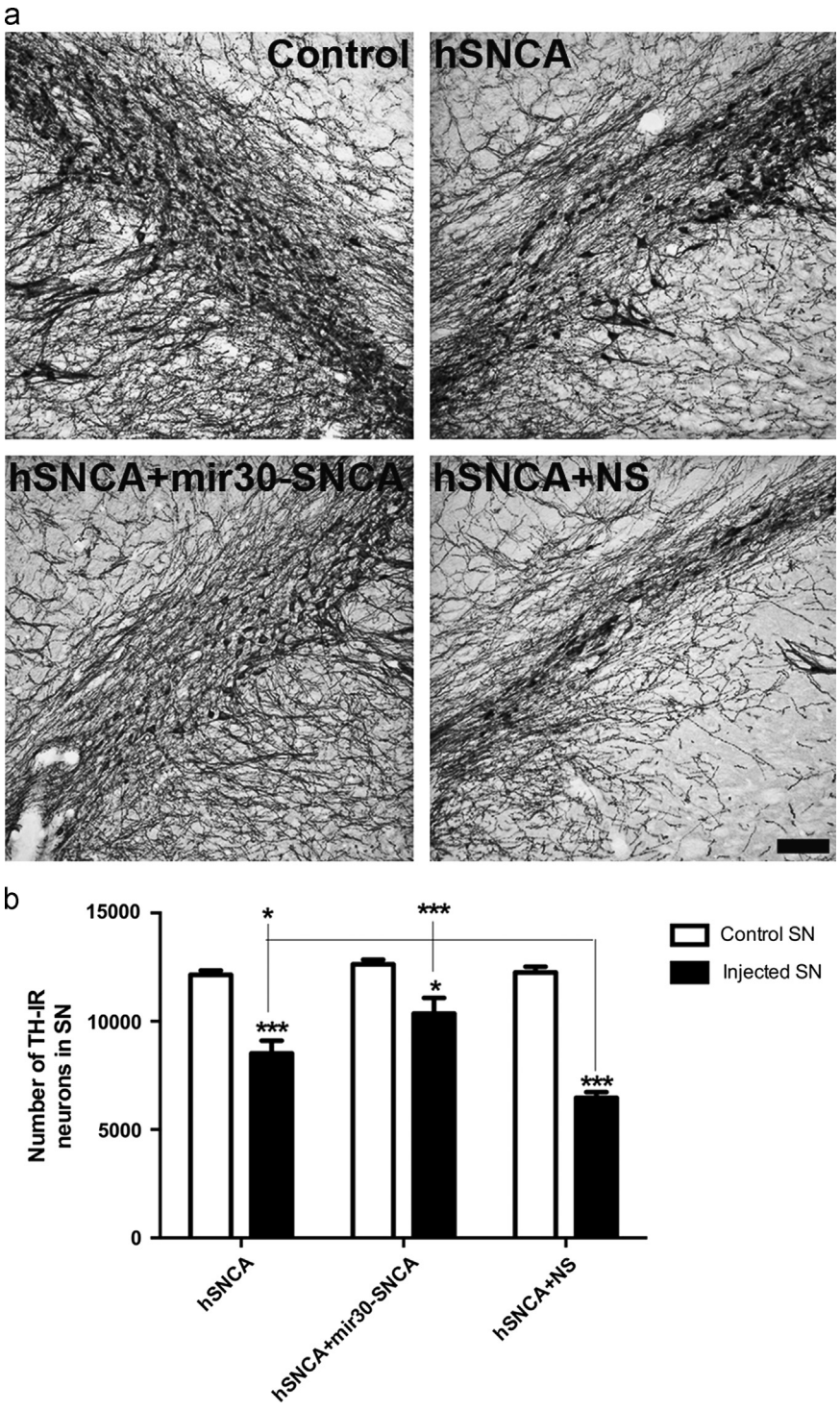

Fig. 4 – hSNCA gene silencing ameliorates loss of TH-IR neurons in rat SN. (a) Representative staining for TH-IR in non-injected, control SN and SN of each treatment group and (b) the number of TH-IR neurons in the entire SN at 2 months using unbiased stereology. Cell counts (Mean ± SEM) are shown for control and injected SN in each treatment group. Asterisks represent statistical differences between control and injected SN unless otherwise noted (*$p \leq 0.05$; ***$p \leq 0.001$). All SNs injected with AAV8-hSNCA exhibit reduced TH-IR counts compared to control SNs. SNCA gene silencing ameliorates this deficit in TH-IR neurons (the difference between injected and control SN is reduced), although this deficit is still present. Co-injection of AAV8-NS exacerbates the deficit in TH-IR neurons in that TH-IR counts in injected SN are significantly reduced when compared to those in hSNCA-injected or hSNCA silenced SN. Size bar: 100 μm.

expression at either time point. However, TH-IR fiber density is reduced in ST of rats co-injected with AAV-hSNCA and either AAV-mir30-SNCA or AAV-NS silencing vector compared to rats injected with AAV-hSNCA (1 month-$p \leq 0.05$; $F_{2,12}=5.731$, $p=0.0179$, 2 month-hSNCA and NS: $p \leq 0.001$, hSNCA and mir30-SNCA: $p \leq 0.05$; $F_{2,14}=24.27$, $p<0.0001$). Partial recovery from the

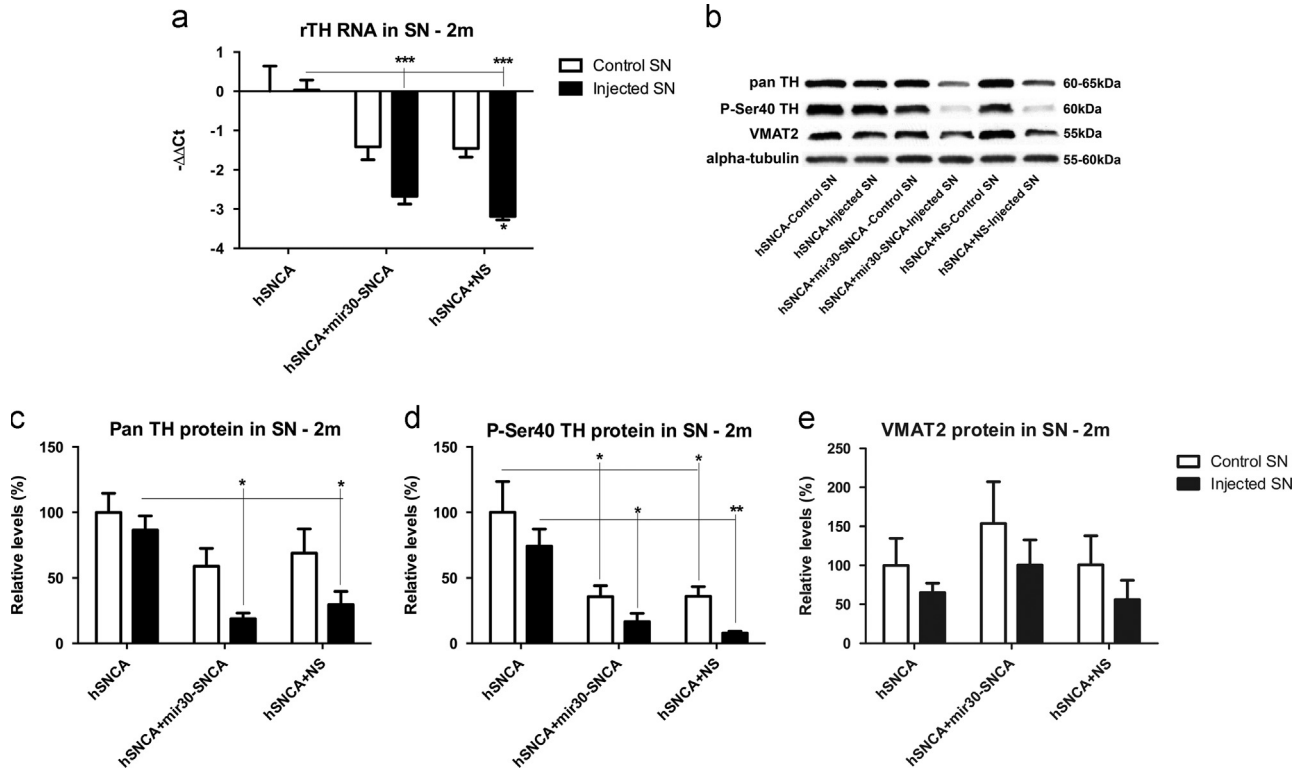

Fig. 5 – Expression of TH, but not VMAT2, is reduced when the silencing construct is co-expressed with hSNCA in the ventral midbrain. The left and right ventral midbrains were dissected from rats 2 months after injection with AAV8-hSNCA, or AAV8-hSNCA with either the AAV8-hSNCA silencing or non-silencing vector (NS). DA phenotypic markers were examined at both the mRNA (a) and protein (b–e) levels. Levels of TH mRNA relative to β-actin mRNA are shown in (a) as $-\Delta\Delta$Ct (mean ± SEM). A representative western blot is shown in (b) and relative levels of TH (c), P-Ser40 TH (d) and VMAT2 (e) protein (compared to alpha-tubulin) are graphed as percent (mean ± SEM). Asterisks represent statistical differences between control and injected unless otherwise noted ($^{*}p \leq 0.05$; $^{**}p \leq 0.01$; $^{***}p \leq 0.001$). Note that at this dose of AAV-hSNCA, there is little overall loss of TH protein or mRNA. However, expression of TH, but not VMAT2, is significantly reduced in rats that received AAV8-hSNCA with either AAV8-silencing vector compared to that in the group that received AAV8-hSNCA alone.

initial reduction in TH fibers (at 1 month) is observed by 2 months after injection in rats in which hSNCA was silenced with mir30-SNCA; ST injected with AAV-hSNCA and AAV-mir30-SNCA have increased fiber density measurements compared to ST injected with AAV-hSNCA and AAV-NS ($p \leq 0.01$), and TH fiber density measurements in ST injected with AAV-hSNCA and AAV-mir30-SNCA at 2 months are greater than those at 1 month ($p \leq 0.05$). However, 2-way ANOVA did not show a significant effect of time, but did show a trend regarding an interaction of time and treatment ($F_{2,26}=2.847$, $p=0.0762$). These data suggest that although expression of silencing vector is toxic to TH-IR fibers, SNCA gene silencing promotes recovery from this initial toxic effect.

2.7. *Expression of either mir30-SNCA or NS silencing vector results in loss of total P-Ser40 TH expression, without loss of VMAT2 in the ST*

To further examine effects of hSNCA expression and silencing on DA fibers in the ST, the left and right ST were dissected from rats injected with AAV-hSNCA, or AAV-hSNCA and either AAV-mir30-SNCA or AAV-NS silencing vector, and DA phenotypic markers were examined at the protein level (Fig. 7). Although all injected ST trend toward reduced levels of TH protein as detected by either the pan TH (Fig. 7b) or Ser40 phosphorylated TH (Fig. 7c) antibodies compared to control ST, these trends are only significant in ST injected with AAV-hSNCA and AAV-NS for pan TH ($p \leq 0.05$; $F_{5,24}=4.333$, $p=0.006$) and in ST injected with AAV-hSNCA and either AAV-mir30-SNCA or AAV-NS silencing vector for P-Ser40 TH ($p \leq 0.01$; $F_{5,24}=8.893$, $p<0.0001$). Similar to the observations in the ventral midbrain, protein levels of VMAT2 (Fig. 7d) are not affected by treatment, suggesting that DA fibers in the ST are equivalent in all groups although TH expression is affected by expression of either mir30-SNCA or NS silencing vector.

2.8. *Co-expression of either mir30-SNCA or NS silencing vector increases inflammation in the SN*

To examine the effect of hSNCA expression and silencing on inflammation, SN sections were stained for Iba-1-IR, which is up-regulated during microglia activation, at both 1 and 2 months (Fig. 8). Qualitatively, a small increase in Iba-1-IR compared to control SN was observed in SN injected with AAV-hSNCA alone. However, a strong inflammatory response in SN, as detected by increased Iba-1-IR was observed in rats injected with either AAV-mir30-SNCA or AAV-NS silencing vector. This increase in Iba-1-IR was the greatest after 1

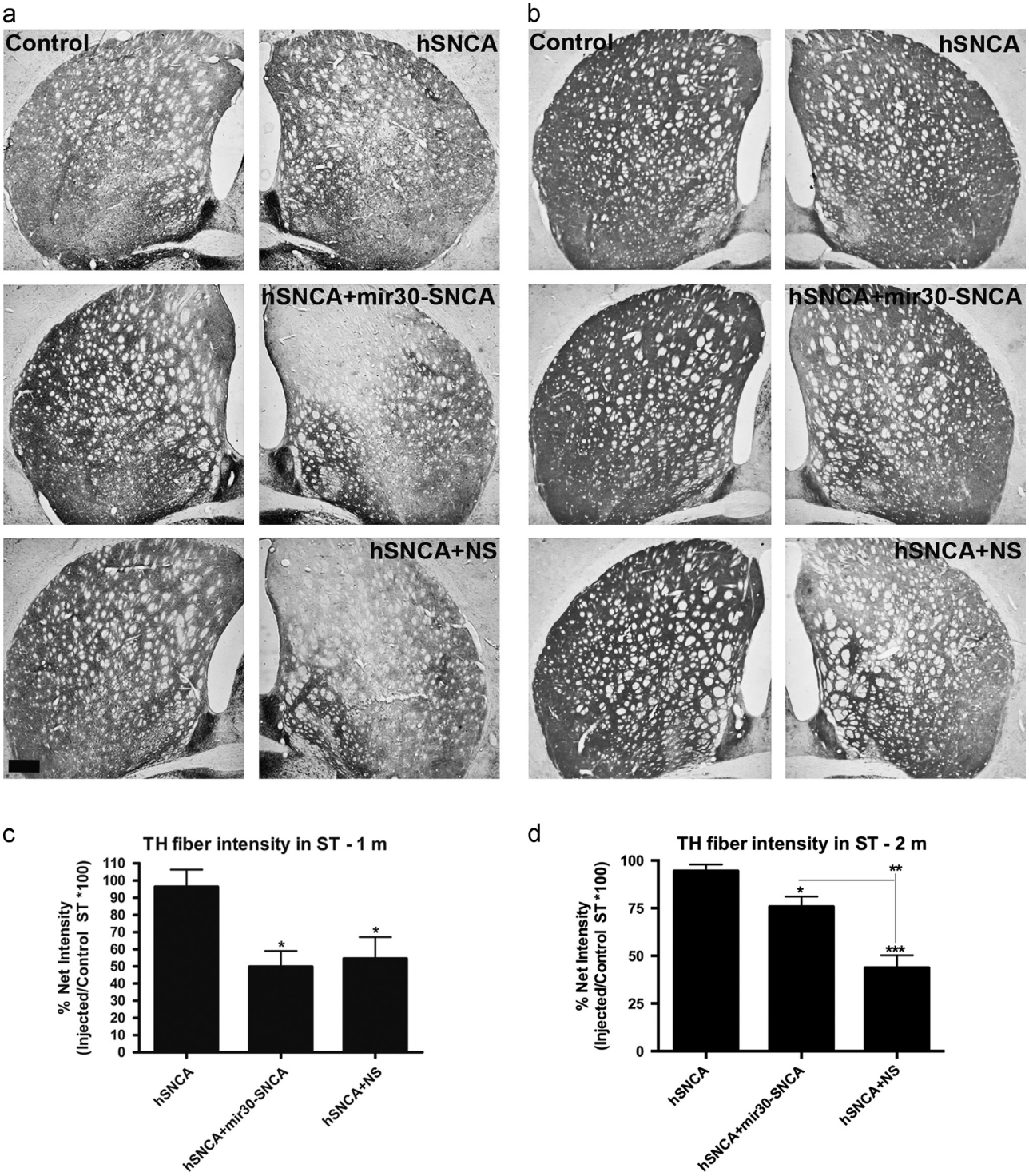

Fig. 6 – TH-IR fibers in ST exhibit recovery by 2 months when hSNCA is silenced. Representative sections showing TH-IR in control ST and ST from rats injected with AAV8-hSNCA alone or AAV8-hSNCA with either silencing vector at 1 (a) or 2 months (b). Density of TH-IR fibers was determined using NIH Image J™ and is graphed as a percent of injected/control (mean ± SEM) at 1month (c) and 2 months (d). Statistical differences are compared to AAV8-hSNCA unless otherwise noted (*$p \leq 0.05$; **$p \leq 0.01$; ***$p \leq 0.001$). Note that there is little loss of TH-IR fibers in ST at this dose of AAV-hSNCA. In contrast, inclusion of either silencing vector leads to a significant loss of TH-IR fibers in ST at 1 month. By 2 months, fiber loss has recovered significantly in rats with silenced hSNCA (2 months, 75.8 ± 5.4 vs. 1 month, 49.8 ± 9.2, $p \leq 0.05$), but TH-IR fibers do not show recovery in rats that received the non-silencing vector. Size bar, 400 μm.

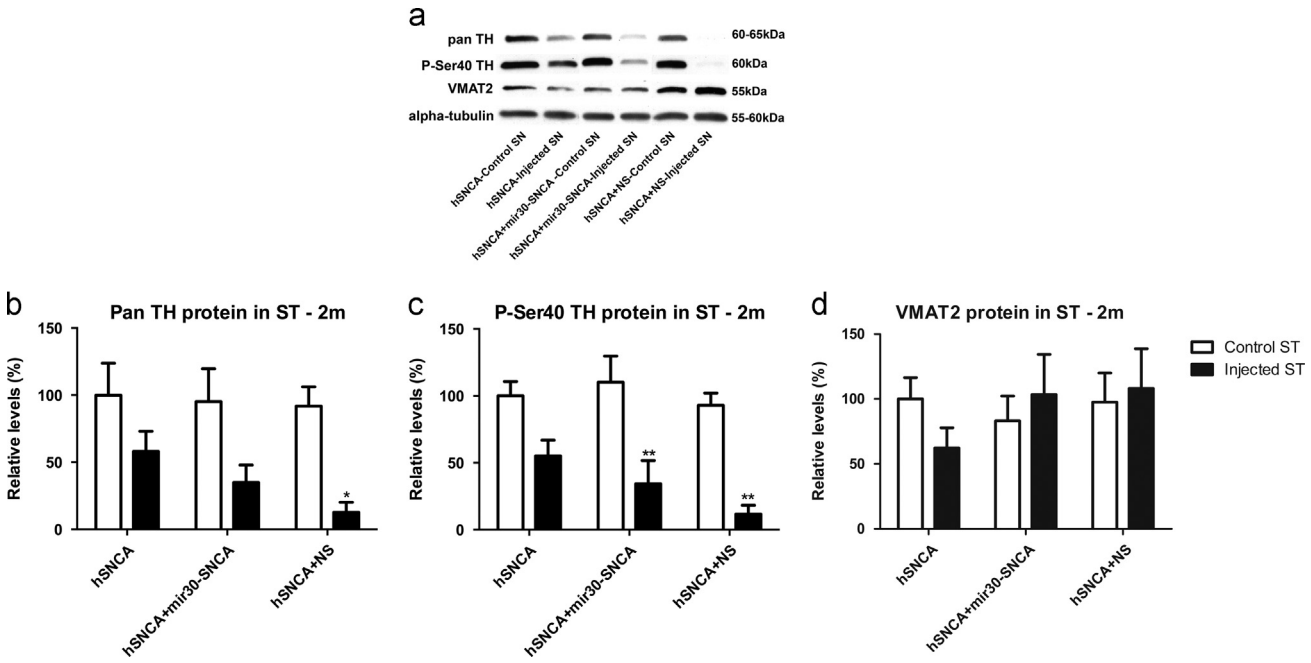

Fig. 7 – Total P-Ser40 TH expression, but not total VMAT2, is reduced in ST injected with either silencing vector. The left and right ST were dissected from rats 2 months after injection of AAV8-hSNCA, or AAV8-hSNCA with either AAV8-silencing vector. DA phenotypic markers were examined at the protein level. A representative western blot is shown in (a) and relative levels of TH (b), P-Ser40 TH (c) and VMAT2 (d) protein expression (compared to alpha-tubulin) are graphed (mean ± SEM). Statistical differences are noted between control and injected ST ($^{*}p \leq 0.05$; $^{**}p \leq 0.01$).

month in SN that received AAV-hSNCA plus AAV-mir30-SNCA. By 2 months, a partial recovery was observed in SN where hSNCA is silenced with mir30-SNCA, although Iba-1-IR remains increased compared to control SN. In contrast, the increased Iba-1-IR observed in SN injected with AAV-hSNCA and AAV-NS remains consistent from 1 to 2 months.

3. Discussion

The aberrant expression of SNCA observed in several diseases termed synucleinopathies, which includes PD, suggests that targeting SNCA for downregulation is a plausible therapeutic approach. We have been investigating whether hSNCA RNAi can protect DA neurons against hSNCA-induced toxicity and functional deficits in a rat model where hSNCA is ectopically expressed in the SN. In the current study, delivery of hSNCA to the rat SN using AAV2/8 induced a deficit in forelimb motor behavior and loss of TH-IR neurons in the SN at 1 month. A mir30-embedded shRNA silencing vector (mir30-SNCA) silenced ectopic hSNCA expression, *in vivo*, in rat SN and ST, which resulted in both positive and negative effects on the nigrostriatal DA system and associated behavior. Positive effects of hSNCA gene silencing included protection against the hSNCA-induced deficit in forelimb motor behavior by 2 months, amelioration of TH-IR cell loss in the SN, partial recovery from initial mir30-SNCA-induced toxicity on TH-IR fibers in the ST and partial recovery from initial mir30-SNCA-induced inflammation in the SN. However, the negative effects of this hSNCA gene silencing included the incomplete protection of TH-IR neurons in the SN, an initial toxic effect on TH-IR fibers in the ST and the presence of inflammation in the SN, as well as reduced total TH expression in the SN and reduced total Ser40 phosphorylated TH in the ST (as measured by western blot). These negative hSNCA gene silencing effects suggest that this hSNCA-specific mir30-embedded shRNA (mir30-SNCA), at the currently examined dose, does not hold potential for development as a clinical therapy.

Apparent inconsistencies between TH expression data in the ventral midbrain as assessed by western blot and TH-IR neuron counts in the SN were observed. These inconsistencies were present in rats that received AAV-mir30-hSNCA with AAV-hSNCA, which show partial protection of TH-IR neuron numbers compared to rats that received AAV-hSNCA alone, but reduced total TH protein, and in rats that received hSNCA alone, which show loss of TH-IR neurons but no effect on total TH expression. These TH inconsistencies are likely explained by differences in production of TH at the cellular level. For example, the protected TH-IR neurons found in the hSNCA-silenced SNs (hSNCA and mir30-SNCA) may express low TH levels per neuron, leading to reduced total TH in the ventral midbrain. On the other hand, compensation for lost TH-IR neurons by increased TH expression in surviving neurons could explain the lack of an effect on total ventral midbrain TH expression observed in rats that received AAV-hSNCA alone.

Two different hSNCA-expressing control groups were used in this study, one that received AAV-hSNCA alone and one that received AAV-hSNCA and a control, non-silencing, silencing vector containing a scrambled sequence (AAV-NS), which interestingly differed in some of the toxic effects examined. Both hSNCA-expressing groups exhibited a similar

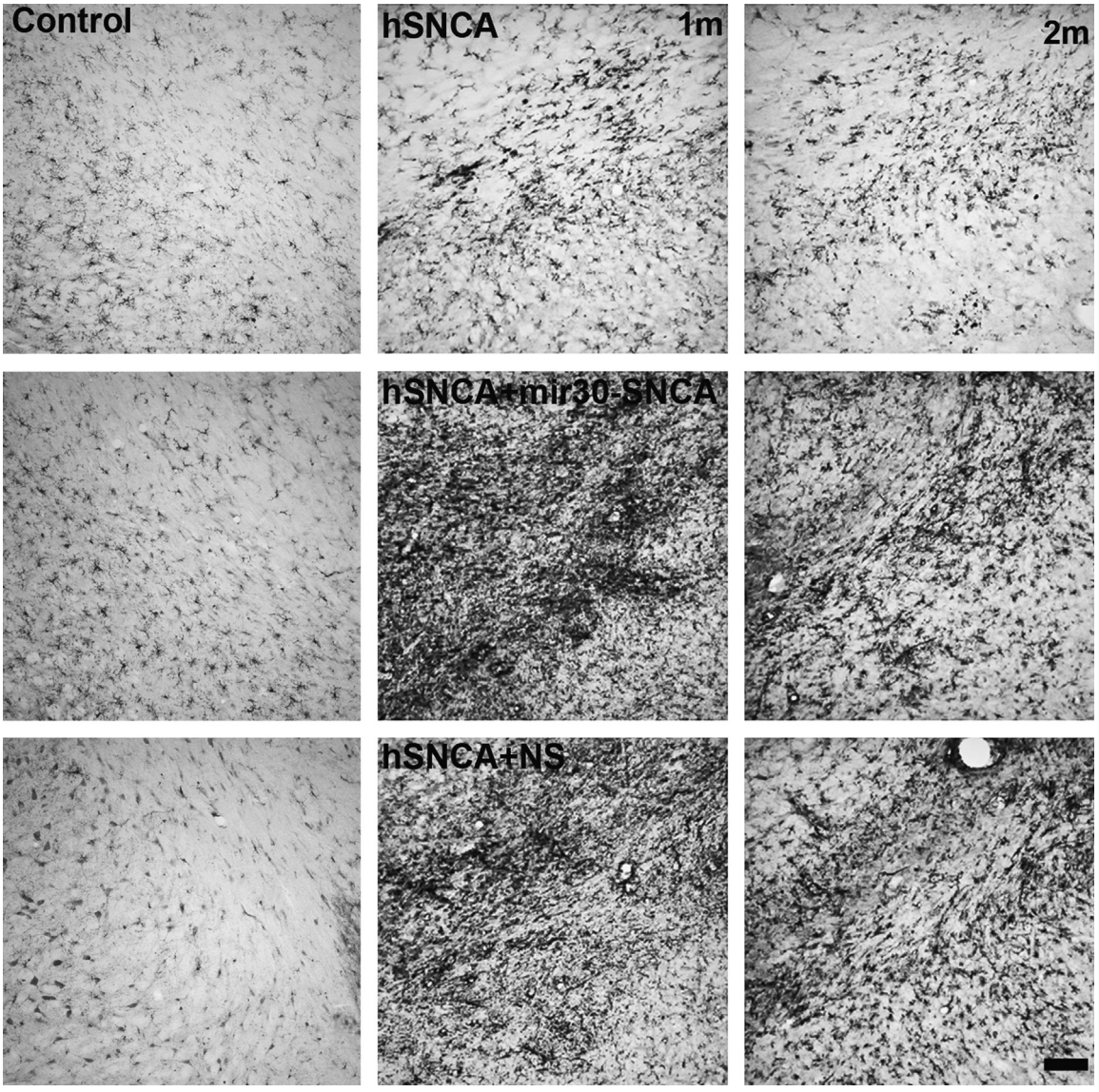

Fig. 8 – Co-expression of silencing vector with AAV8-hSNCA induces an inflammatory response in the SN. Brain sections stained for Iba-1 as a marker for microglia are shown in control SN (left panels) and in AAV8-hSNCA-, AAV8-hSNCA+AAV8-mir30-SNCA- and AAV8-hSNCA+AAV8-NS-injected SN at 1month (middle panels) and 2 months (right panels). Note that Iba-1-IR is very high in SN of rats injected with either silencing vector and that although this is somewhat reduced by 2 months, it remains higher than in rats injected with AAV-hSNCA alone. Size bar: 100 μm.

forelimb motor deficit and similar loss of TH-IR neurons in the SN by 1 month. However, rats that received AAV-hSNCA and AAV-NS exhibited greater toxic effects than those observed in rats that received AAV-hSNCA alone, which included loss of TH-IR fibers in the ST, reduction in total TH expression in the ventral midbrain and the ST, as measured by western blot, and an increased inflammatory response as detected by Iba-1-IR. The greater toxicity observed in rats treated with AAV-hSNCA and AAV-NS could be attributed to silencing vector design, off-target effects of the scrambled sequence, or to increased viral load. It is also possible that co-injection of silencing vector resulted in some unknown modulatory effect on hSNCA vector expression. Rats that received hSNCA alone did exhibit some reduction in total TH expression in the ventral midbrain and ST, as measured by western blot, although this reduction was not significant. A lack of toxicity on TH-IR fibers in the ST by AAV2/8-hSNCA alone, has also been observed in some studies where hSNCA was delivered to the SN using either AAV2/6 (Azeredo da Silveira et al., 2009) or AAV2/8 (McFarland et al., 2009). However, other studies using AAV2/2, 2/5 or 2/6 have shown hSNCA-induced reductions in TH-IR fibers in the ST by 8 weeks (Decressac et al., 2012; Gorbatyuk et al., 2008; Kirik et al., 2002; Lundblad et al., 2012). These differences most likely reflect varying levels of hSNCA protein in DA axons due to differences in vector dose, serotype and/or efficiency of retrograde transport, but may also result from toxic effects at different ST levels since only one ST level was quantified. The AAV-hSNCA and AAV-NS group is the most appropriate hSNCA-expressing control group for assessment of effects

due to hSNCA gene silencing with mir30-SNCA because both of these groups received similar viral load and were injected with similar vector constructs. When compared to the AAV-hSNCA and AAV-NS group, hSNCA gene silencing with mir30-SNCA results in significant protective effects on forelimb motor behavior, TH-IR neurons in the SN and TH-IR fibers in the ST. However, toxic effects that may have resulted from high viral load or from silencing vector design were observed in both the NS and mir30-SNCA groups. These negative effects include reductions in total TH in the ventral midbrain and in P-Ser40 TH in the ST, as well as the presence of inflammation in the SN, even though an apparent qualitative recovery from inflammation was observed after hSNCA gene silencing with mir30-SNCA (1 month survival vs. 2 month survival).

As discussed, silencing of hSNCA using mir30-SNCA ameliorated some toxic effects observed in hSNCA-expressing rats. Of these positive hSNCA gene silencing effects, the protection against the hSNCA-induced forelimb deficit is of particular interest because it appears to be due specifically to silencing hSNCA in DA terminals in the ST. At 2 months after injection, expression of hSNCA in the ST correlated with the deficit in contralateral forelimb use. Possible correlation of these measures was not assessed at 1 month because the survival time for all rats in this portion of the study was 2 months. hSNCA mRNA may have been silenced either at the terminals or in the cell body, thereby reducing transport of hSNCA mRNA to the ST. Our data suggest that the presence of hSNCA with either silencing vector induces loss of TH fibers in the ST. Importantly, hSNCA gene silencing promotes a partial recovery from this initial toxic effect on TH-IR fibers in the ST, which is not observed in the AAV-NS control group. This partial protection of TH-IR fibers in rats where hSNCA was silenced also correlates with the recovery in forelimb behavior between 1 and 2 months in this group. These findings are in agreement with our previous study in which a hSNCA-specific shRNA was used to silence hSNCA. In that study, not only was there a protection of forelimb use, but data from fluorogold tract tracing suggested that hSNCA gene silencing promoted sprouting of new nigrostriatal fibers from surviving nigral DA neurons (Khodr et al., 2011). Sprouting may also have occurred in the current study, although we cannot rule out the possibility that partial recovery in TH protein in ST also contributed to behavioral improvement.

Although hSNCA gene silencing with mir30-SNCA exhibited positive effects, the observed negative effects exclude the current dose of mir30-SNCA from further preclinical development. The negative effects may have been due to expression of the silencing construct or to viral dose. Toxicity on midbrain DA neurons due to high viral loads or high transgene expression also has been observed by others. Ulusoy et al. (2009) observed that high titer AAV5 vectors expressing either an shRNA or GFP induced loss of DA neurons, as well as microglial activation, and Koprich et al. (2010, 2011) observed that high titer AAV1/2 expressing GFP induced loss of SN neurons. However, in the current study, differences were observed between rats injected with AAV-hSNCA and AAV-mir30-hSNCA and rats injected with AAV-hSNCA and AAV-NS even though both groups received similar doses of vectors. Moreover, effects were significantly better in rats in which hSNCA was silenced compared to NS control rats.

It is possible that a lower ratio of mir30-SNCA to hSNCA could reduce some of the observed negative effects either due to reduced silencing vector expression or reduction of viral load. Further preclinical testing of different vector ratios and the effects of silencing vector alone might lead to identifying a viable path to the clinic for SNCA gene silencing. A conundrum with attempting to resolve the problem of viral load is that reducing delivery of hSNCA may result in a lack of hSNCA-induced toxicity and reducing delivery of silencing vector may not silence hSNCA enough to produce protective effects. Our current data suggest that a lower dose of this mir30-hSNCA would result in incomplete gene silencing and reduced behavioral protection at 1 month. However, long-term dose studies may reveal greater behavioral protective effects by lower doses of silencing vector. For example, protection of forelimb motor behavior at the 1:55 dose examined in the current experiments did not occur until 2 months when both ipsilateral and contralateral paws were used to similar extents (Fig. 3), even though ipsilateral and contralateral forelimb use was significantly different from respective hSNCA-induced forelimb use at 1 month (Fig. 1). Another approach to reduce possible toxicity due to high viral load might be to express mir30-SNCA under a stronger or cell-specific promoter. Alternatively, AAV-mir30-SNCA could be tested in other models where hSNCA and silencing vector expression are uncoupled in order to prevent possible undesired modulatory effects of silencing vector virus on delivery or expression of AAV-hSNCA, such as transgenic hSNCA mouse models that present with behavioral and midbrain DA neuron deficits (Masliah et al., 2000; Richfield et al., 2002). However, symptoms in these transgenic models do not become evident until 12 months, a serious drawback compared to the rapid degeneration model used in the current study.

The findings presented in this paper reveal positive and negative effects of hSNCA silencing vector expression in the rat SN and suggest that gene silencing using this AAV2/8-mir30-hSNCA construct, although promising *in vitro*, is not a candidate for therapeutic translation for PD at the currently tested dose. However, the observed partial protective effects of this silencing vector on DA neurons and motor function suggest that further modification of vector design may provide a more promising silencing vector outcome, perhaps by expressing the silencing sequence under a stronger promoter so that a lower viral load can be used and/or by designing silencing sequences that minimize potential and undesirable off target effects.

4. Experimental procedures

4.1. *Generation of adeno-associated viral (AAV) shuttle plasmids and virus packaging*

Shuttle plasmids pAAV-CBA-hSNCA, pAAV-mir30-non-silencing (NS) and pAAV-mir30-SNCA were cloned as previously described (Han et al., 2011; Khodr et al., 2011). Expression cassettes were confirmed by sequencing and vectors were packaged as serotype AAV2/8 by the University of Pennsylvania Vector Core. Viral titers were: AAV-CBA-hSNCA – 6.22×10^{13} vector genomes (vg)/ml, AAV-mir30-NS – 1.85×10^{14} vg/ml, AAV-mir30-SNCA – 1.76×10^{14} vg/ml.

4.2. Animals

Adult male Sprague Dawley rats weighing 175–200 g were purchased from Harlan laboratories (Indianapolis, IN) and housed in the Children's Hospital of Chicago Research Center animal facility on a 12 h light/dark cycle with food and water available ad libitum. Animal care and use procedures were conducted in accordance with NIH, USDA and institutional guidelines.

4.3. Treatment groups and sample sizes

An initial vector dose response study was carried out with a 1 month survival using 48 rats to determine the optimal dilution of AAV2/8-hSNCA and ratio of AAV2/8-hSNCA to silencing vector for use in efficacy experiments (Table S1). For the behavioral study, treatment groups were: AAV- hSNCA alone ($n=16$ at 1 month; $n=11$ at 2 months); AAV-hSNCA and AAV-NS ($n=15$ at 1 month and 10 at 2 months); AAV-hSNCA and AAV-mir30-SNCA ($n=16$ at 1 month and $n=11$ at 2 months). At 1 month, rats were sacrificed for histological analysis of TH-IR fiber density in ST and Iba-1 in SN ($n=5$). The remaining rats were sacrificed at 2 month with half the rats prepared for histology and half for molecular analyses ($n=5$–6). A separate group of rats was injected for molecular analysis at 10 days ($n=3$).

4.4. Stereotaxic surgery and post-operative animal care

The skin overlying the skull of isoflurane-anesthetized rats was shaved. Stereotaxic surgeries were carried out using a Stoelting stereotaxic apparatus equipped with a Stoelting quintessential stereotaxic injector holding a 10 μl Hamilton syringe with a 26 gauge needle. A hole was drilled in the skull over the appropriate injection site at stereotaxic coordinates, 5.5 mm posterior, −1.9 mm lateral and 7.4 mm ventral from Bregma (SN injection). The syringe was inserted into the brain at a speed of ~1 mm/min and then allowed to remain in place for 2 min before vector injection. 2 μl of each virus mixture was injected at a rate of 0.5 μl/min into one SN, and the needle was left in place for 5 min at the end of the injection in order to minimize diffusion up the needle track. The doses of each vector used for the dose response experiments are shown in Table S1. For the efficacy experiment, rats received 6.22×10^{9} vg of AAV2/8-hSNCA alone or with either 3.51×10^{11} vg of AAV2/8-mir30-NS or 3.26×10^{11} vg of AAV2/8-mir30-SNCA in a 2 μl volume. The syringe was withdrawn at a rate of ~1 mm/min. The drill hole was plugged with gel foam to control bleeding and Marcaine was spread around the surgical site. The skin was sutured and treated with topical antibiotic ointment and rats were returned to the vivarium upon recovery from anesthesia. Twenty-four hours after surgery, rats were transferred to a clean cage and the old bedding was autoclaved.

4.5. Non-drug induced forelimb motor behavior

Rats were placed inside of a plexiglass cylinder, partially surrounded by mirrors in a quiet, dark room. The activity of each rat was recorded on videotape under red light for a 10 min period. The number of times each paw was used for wall touches on the first 25 rearings of each rat was counted by an observer blinded to treatment group to determine forelimb use preference as previously published (Schallert et al., 2000). All treated rats underwent forelimb behavior testing at 1 month or at both 1 and 2 months after vector injection.

4.6. Tissue preparation

For molecular analyses, rats were anesthetized with sodium pentobarbital (75 mg/kg) and perfused through the ascending aorta with 0.9% saline. The left and right ventral mesencephalons, as well as the left and right striata were collected and stored at −80 °C until homogenization. To extract nucleic acids and the soluble protein fractions, tissues were homogenized in homogenization buffer (1× PBS, 1% Triton-Tx, 5 mM EDTA) containing 10 μl/ml of HALT protease and phosphatase inhibitor (Thermo Scientific) using a glass homogenizer. After 4 freeze-thaw cycles in an ethanol bath at −80 °C for 2 min and a 37 °C water bath for 2 min, homogenates were centrifuged at 100,000 × *g* for 1hr at 4 °C. The supernatant was collected and the pellet (ribosomal mRNA, DNA, insoluble protein) was suspended in TRI Reagent™ (Ambion, Austin, TX). The TRI protocol was used to extract RNA and DNA.

For histology, sodium pentobarbital-anesthetized rats were perfused through the ascending aorta with 0.9% saline containing 0.002% sodium nitrite, followed by 4% phosphate buffered paraformaldehyde (pH=7.4). Brains were post-fixed overnight in 5% sucrose–4% paraformaldehyde and then cryoprotected in an increasing gradient of sucrose concentrations (10–30%) in 0.1 M PBS. A sliding microtome (Leica SM2000 R) was used to cut sections in the coronal plane at 40 μm. Six serial sets of sections were collected and stored in cryoprotectant solution at −20 °C.

4.7. QPCR

TRI-extracted RNA was treated with a DNase before quantitation. RNA and DNA levels were measured using quantitative TaqMan™ or SYBR Green real-time PCR on an Applied Biosystems (Foster City, CA) 7500 fast real-time PCR system. TaqMan RNA reactions contained 25 ng of RNA, 12.5 μl of 2× TaqMan Universal PCR buffer, 6.25 U of MuLV reverse transcriptase, 1.25 U of RNase inhibitor, 0.25 μl of each primer (10 μM forward β-actin, TH, or 20 μM forward hSNCA and 20 μM reverse β-actin, hSNCA or 10 μM reverse TH), and 0.5 μl of probe (5 μM) in a 25 μl volume. TaqMan DNA reactions contained the same components as the RNA reactions, except water replaced the reverse transcriptase and RNase inhibitor. For DNA, only hSNCA plasmid content was measured using TaqMan real-time PCR. SYBR Green real-time PCR was used to measure turbo GFP plasmid (i.e. silencing vector) content. SYBR Green reactions contained 25 ng of DNA, 12.5 μl of 2× Power SYBR Green Master Mix, 0.25 μl of AmpErase and 2.25 μl of each primer (10 μM) in a 25 μl volume. Target-specific primers and probes were designed using Primer Express 3.0 (Applied Biosystems) and BLAST (blast.ncbi.nlm.nih.gov). Primers and probes used are as follows: hSNCA (fwd primer: GACCAGTTGGGCAAGAATGAAG, rev primer: GGTTCGTAGTCTTGATACCCTTCCT, probe: TCTGGAAGATATGCCTGTGGATCCTGACA); rat TH (fwd primer: CGGAAGAGATTGCTACCTGGAA,

rev primer: GTAGCCACAGTACCGTTCCAGAA, probe: TCACGCTGAAGGGCCTCTATGCTACC; rat β-actin (fwd primer: TCACCCCTGTGCCCATCTATG, rev primer: CATCGGAACCGCTCATTGCCGATAG, probe: ACGCGCTCCCTCATGCCATCCTGCGT); and turbo GFP (fwd primer: AGCGTGATCTTCACCGACAAG, rev primer: CTGCCATCCAGATCGTTATCG). Probes contained a FAM reporter dye and a QSY7 quencher dye, except for the hSNCA probe, which contained a BHQ1 quencher dye. Reactions were incubated at 48 °C for 30 min, 95 °C for 10 min, then 40 cycles of 95 °C for 15 s and 59 °C for 1 min. Data are expressed as delta Ct compared to β-actin Ct and compared to the control SN in the group of rats treated with hSNCA.

4.8. Western blots

Protein levels in the soluble fraction were measured using the Bio-Rad DC protein assay kit (500-0111). Samples containing 25 μg of total protein were separated by SDS-PAGE on 4–15% Tris HCl gels and transferred to PVDF membranes (Millipore) at 12 V for 1 h. Membranes were blocked with 5% blocking reagent for 1 h at room temperature, then incubated in primary antibody overnight at 4 °C (1:2000 rabbit anti-P Ser40 TH; 1.25 μg/ml rabbit anti-VMAT2, Millipore, Billerica, MA) or for 1hr at room temperature (1:2500 rabbit anti-pan TH, Millipore; 1:10,000 mouse anti-α-tubulin, Sigma). After washes, membranes were incubated for 1hr at room temperature in horseradish peroxidase (HRP)-conjugated goat anti-mouse or goat anti-rabbit secondary antibody (1:5000, Santa Cruz, CA). Membranes were developed using Supersignal West Pico Luminol/enhanced solution and West Pico stable peroxide solution (Pierce, Appleton, WI), and exposed to Kodak BioMax Light Film. Films were scanned as 600 dpi grayscale tiff images using a CanoScan8400F flatbed scanner, and net intensities of bands were measured using Carestream MI SE software.

4.9. Immunohistochemistry

Free-floating tissue sections were rinsed of cryoprotectant solution. For diaminobenzidine (DAB) staining, tissue sections were incubated in H_2O_2 in order to quench endogenous peroxidase activity. Sections were blocked in normal goat serum (NGS) for 1hr to minimize nonspecific antibody binding and then incubated overnight at room temperature in primary antibody (for fluorescence: 1:50 mouse anti-hSNCA, Invitrogen; for DAB: 1:2000 rabbit anti-pan TH, or 1.5 μg/ml rabbit anti-Iba-1, Wako). After rinses, sections were incubated in an appropriate secondary antibody (1:100 Cy3-conjugated goat anti-mouse; 1:200 Cy2-conjugated goat anti-rabbit, Jackson Immunoresearch, West Grove, PA; or, 1:500 biotinylated goat anti-rabbit IgG, Vector Laboratories) for 2.5 h at room temperature. For fluorescence staining, sections were mounted on slides, air dried overnight, and coverslipped with Fluorosave (Calbiochem, La Jolla, CA). For DAB staining, sections were rinsed and incubated with avidin-biotinylated enzyme complexes (Vector Laboratories) for 2 h at room temperature and developed using a DAB solution (50 mM sodium acetate, 10 mM imidazol, 0.4 mg/ml DAB, 0.005% H_2O_2) containing or not containing 0.5 g/ml nickel sulfate. Sections were mounted on slides, dried overnight, dehydrated and coverslipped. Slides were evaluated using a Leica DMR upright microscope equipped for epifluorescence microscopy.

4.10. DA marker fiber measurements in ST

ST sections were stained for TH immunoreactivity (IR) using nickel enhancement and slides were scanned as 600 dpi, 8 bit grayscale tiff images using a CanoScan8400F flatbed scanner with automatic settings disabled. One section at the level of the anterior commissure (−0.26 mm from Bregma) was chosen from each brain for fiber density measurement. Using Fiji software (http://imageJ.nih.gov/ij), each ST was outlined using the freehand tool, processed to correct for background and brightness, converted to a binary image and the number of pixels in the ST determined as a measure of TH-IR fiber density. ST fiber density data are expressed as a percentage of injected vs control ST for each treatment group.

4.11. TH cell counts

Sections of SN were stained for TH-IR without nickel enhancement. For the dose response study, the number of TH-IR neurons was counted in both injected and control SNs in one section from each brain at the level of the medial terminal nucleus accessory optic tract (−5.3 mm from Bregma) using Neurolucida software (Micro Bright Field Biosciences).

For the efficacy study, unbiased stereology was used to determine the total number of TH-IR neurons in each SN. Seven sections at similar anterior to posterior levels were chosen throughout the anterior-posterior extent of the SN in every brain. The number of TH-IR cells was counted in injected and control SN using StereoInvestigator™ software (Micro Bright Field Biosciences). Parameters were as follows: grid size (80 × 80), frame size (175 × 175), guard zones (3 μm), optical dissector height (10 μm). The Gundersen coefficient of error was ≤ 0.07 for TH neuronal counts in the control SN and ≤ 0.11 for TH neuronal counts in experimental SN.

For both counting methods, only large TH-IR neurons (greater than ~15 μm in diameter) were counted to avoid counting interneurons or dying neurons.

4.12. Imaging

Histology images were collected using a Retiga 4000R digital camera on a Leica DMR upright microscope. Adobe Photoshop CS5 was used to compile multi-photo plate figures.

4.13. Statistical analysis

Data were analyzed using Prism software. Kruskal–Wallis one-way ANOVAs followed by Dunn's post hoc tests were used to compare treatment groups for forelimb behavior analysis. All other data were analyzed using a parametric one-way ANOVA followed by Tukey's post hoc tests. Statistically significant differences were set at $p \leq 0.05$. Data are expressed as mean ± SEM.

Acknowledgments

This study was supported by the Department of Defense Neurotoxicology Program (NO06079001) and NIH grants (NS31957 and NS054989 to M.C.B. and T32 NS041234 to C.E.K.),

the Harry F. and Elaine M. Chaddick Foundation and the Medical Research Institute Council of Ann and Robert H. Lurie Children's Hospital of Chicago. The University of Pennsylvania Viral Vector Core is acknowledged for AAV production. The technical assistance of Jianping Xie and Brian Corstange (Ann and Robert H. Lurie Children's Hospital of Chicago Research Center) and technical advice of Hemraj Dodiya (Rush University) is appreciated. M.C.B. holds European and U.S. patents on this technology.

Appendix A. Supporting information

Supplementary data associated with this article can be found in the online version at http://dx.doi.org/10.1016/j.brainres.2014.01.010.

REFERENCES

Azeredo da Silveira, S., et al., 2009. Phosphorylation does not prompt, nor prevent, the formation of alpha-synuclein toxic species in a rat model of Parkinson's disease. Hum. Mol. Genet. 18, 872–887.

Boudreau, R.L., Monteys, A.M., Davidson, B.L., 2008. Minimizing variables among hairpin-based RNAi vectors reveals the potency of shRNAs. RNA 14, 1834–1844.

Boudreau, R.L., Martins, I., Davidson, B.L., 2009. Artificial microRNAs as siRNA shuttles: improved safety as compared to shRNAs in vitro and in vivo. Mol. Ther. 17, 169–175.

Castanotto, D., et al., 2007. Combinatorial delivery of small interfering RNAs reduces RNAi efficacy by selective incorporation into RISC. Nucleic Acids Res. 35, 5154–5164.

Chesselet, M.F., 2008. In vivo alpha-synuclein overexpression in rodents: a useful model of Parkinson's disease?. Exp. Neurol. 209, 22–27.

Decressac, M., et al., 2012. Progressive neurodegenerative and behavioural changes induced by AAV-mediated overexpression of alpha-synuclein in midbrain dopamine neurons. Neurobiol. Dis. 45, 939–953.

Fire, A., et al., 1998. Potent and specific genetic interference by double-stranded RNA in *Caenorhabditis elegans*. Nature 391, 806–811.

Gorbatyuk, O.S., et al., 2008. The phosphorylation state of Ser-129 in human alpha-synuclein determines neurodegeneration in a rat model of Parkinson disease. Proc. Natl. Acad. Sci. U.S.A. 105, 763–768.

Grimm, D., et al., 2006. Fatality in mice due to oversaturation of cellular microRNA/short hairpin RNA pathways. Nature 441, 537–541.

Han, Y., et al., 2011. A microRNA embedded AAV alpha-synuclein gene silencing vector for dopaminergic neurons. Brain Res. 1386, 15–24.

Hayashita-Kinoh, H., et al., 2006. Down-regulation of alpha-synuclein expression can rescue dopaminergic cells from cell death in the substantia nigra of Parkinson's disease rat model. Biochem. Biophys. Res. Commun. 341, 1088–1095.

Khodr, C.E., et al., 2011. An alpha-synuclein AAV gene silencing vector ameliorates a behavioral deficit in a rat model of Parkinson's disease, but displays toxicity in dopamine neurons. Brain Res. 1395, 94–107.

Kirik, D., et al., 2002. Parkinson-like neurodegeneration induced by targeted overexpression of alpha-synuclein in the nigrostriatal system. J. Neurosci. 22, 2780–2791.

Kirik, D., et al., 2003. Nigrostriatal alpha-synucleinopathy induced by viral vector-mediated overexpression of human alpha-synuclein: a new primate model of Parkinson's disease. Proc. Natl. Acad. Sci. U.S.A. 100, 2884–2889.

Koprich, J.B., et al., 2010. Expression of human A53T alpha-synuclein in the rat substantia nigra using a novel AAV1/2 vector produces a rapidly evolving pathology with protein aggregation, dystrophic neurite architecture and nigrostriatal degeneration with potential to model the pathology of Parkinson's disease. Mol. Neurodegener. 5, 43.

Koprich, J.B., et al., 2011. Progressive neurodegeneration or endogenous compensation in an animal model of Parkinson's disease produced by decreasing doses of alpha-synuclein. PLoS One 6, e17698.

Lee, V.M., Trojanowski, J.Q., 2006. Mechanisms of Parkinson's disease linked to pathological alpha-synuclein: new targets for drug discovery. Neuron 52, 33–38.

Lewis, J., et al., 2008. In vivo silencing of alpha-synuclein using naked siRNA. Mol. Neurodegener. 3, 19.

Lo Bianco, C., et al., 2002. Alpha-synucleinopathy and selective dopaminergic neuron loss in a rat lentiviral-based model of Parkinson's disease. Proc. Natl. Acad. Sci. U.S.A. 99, 10813–10818.

Lundblad, M., et al., 2012. Impaired neurotransmission caused by overexpression of alpha-synuclein in nigral dopamine neurons. Proc. Natl. Acad. Sci. U.S.A. 109, 3213–3219.

Marti, M.J., Tolosa, E., Campdelacreu, J., 2003. Clinical overview of the synucleinopathies. Mov. Disord. 18 (Suppl. 6), S21–S27.

Masliah, E., et al., 2000. Dopaminergic loss and inclusion body formation in alpha-synuclein mice: implications for neurodegenerative disorders. Science 287, 1265–1269.

McBride, J.L., et al., 2008. Artificial miRNAs mitigate shRNA-mediated toxicity in the brain: implications for the therapeutic development of RNAi. Proc. Natl. Acad. Sci. U.S.A. 105, 5868–5873.

McCormack, A.L., et al., 2010. Alpha-synuclein suppression by targeted small interfering RNA in the primate substantia nigra. PLoS One 5, e12122.

McFarland, N.R., et al., 2009. Alpha-synuclein S129 phosphorylation mutants do not alter nigrostriatal toxicity in a rat model of parkinson disease. J. Neuropathol. Exp. Neurol. 68, 515–524.

Richfield, E.K., et al., 2002. Behavioral and neurochemical effects of wild-type and mutated human alpha-synuclein in transgenic mice. Exp. Neurol. 175, 35–48.

Sapru, M.K., et al., 2006. Silencing of human alpha-synuclein in vitro and in rat brain using lentiviral-mediated RNAi. Exp. Neurol. 198, 382–390.

Schallert, T., et al., 2000. CNS plasticity and assessment of forelimb sensorimotor outcome in unilateral rat models of stroke, cortical ablation, parkinsonism and spinal cord injury. Neuropharmacology 39, 777–787.

Scherr, M., Eder, M., 2007. Gene silencing by small regulatory RNAs in mammalian cells. Cell Cycle 6, 444–449.

Sibley, C.R., et al., 2012. Silencing of Parkinson's disease-associated genes with artificial mirtron mimics of miR-1224. Nucleic Acids Res. 40 (19), 9863–9875.

Spillantini, M.G., et al., 1997. Alpha-synuclein in Lewy bodies. Nature 388, 839–840.

Ulusoy, A., et al., 2009. Dose optimization for long-term rAAV-mediated RNA interference in the nigrostriatal projection neurons. Mol. Ther. 17, 1574–1584.

Yi, R., et al., 2005. Overexpression of exportin 5 enhances RNA interference mediated by short hairpin RNAs and microRNAs. RNA 11, 220–226.

Yuan, B., Sierks, M.R., 2009. Intracellular targeting and clearance of oligomeric alpha-synuclein alleviates toxicity in mammalian cells. Neurosci. Lett. 459, 16–18.